Available online at www.sciencedirect.com

ScienceDirect

Procedia CIRP 46 (2016) 234 – 237

www.elsevier.com/locate/procedia

7th HPC 2016 – CIRP Conference on High Performance Cutting

Thermal finite-difference modeling of machining operations in polymers

Frédéric Rossi[a]*, Thomas Baizeau[a], Carole Moureaux[a]

[a]*Arts et Metiers ParisTech, LaBoMaP, rue porte de Paris, 71250 Cluny, France*

* Corresponding author. Tel.: +33385595344; fax: +3385595350. *E-mail address:* frederic.rossi@ensam.eu

Abstract

Polymer materials are known to be easily damaged by temperature reached during machining operations. A two-dimensional finite-difference model is established to predict the temperature in orthogonal cutting. Calculations are validated with experiments carried out on polyurethane samples with various cutting speeds and depths of cut. The cutting temperatures are measured by thermocouples embedded within the workpiece and the tool cutting edge. The model provides a three dimensional thermal field of the workpiece with an accuracy of 20 K.

Peer-review under responsibility of the International Scientific Committee of 7th HPC 2016 in the person of the Conference Chair Prof. Matthias Putz

Keywords: Temperature; Simulation; Measurement.

1. Introduction

The temperature at the cutting zone is investigated since the beginning of machining researches and is one of the main affecting parameters for surface integrity and lifetime of tools [1,2]. The heat produced both by shearing and by friction, at the tool tip, may leads, in the case of polymers, to temperatures that can damage the material [3]. Most research works have been conducted on metals and composite materials [4,5] with both the experimental and numerical point of views. Only few papers study the thermal aspect of the cut in thermoplastics [6].

As presented by Arrazola [7],and Klocke [8] most thermal model are performed through an analytical approach. The aim of this study is to establish a model of temperature of the tool, the chip and the piece during planing operations. The limit cutting conditions are estimated by the modelled temperature in the workpiece.

A two dimensional thermal finite difference methodology is developed to model the temperature. In order to improve the accuracy of results, the experimental mechanics data are used as input in the modelling.

Finally, the validation of the model is done with temperature measurements at the tool edge.

2. Experimental set-up

The thermal model needs to be validated with experimental data. Most of the machining involve 3D cutting operations. To simplify the analysis, the problem is reduced to orthogonal cutting configuration. The tool edge–material pair can then be used by recomposing parts of the thermal load for the whole edge on the machined surface.

The experiments are performed in planing operations. The cutting motion is obtained with the longitudinal axis of a DMG DMC85V 3 axis milling machine [9] driven by linear motors. Figure 1 shows the experimental set-up with the cutting tool on the translating x-axis. The machined part is clamped on a Kistler 9119AA2 piezoelectric dynamometer for cutting forces measurements (F_c) and thrust force (F_D). The thermoplastic polymer samples were 4 mm width (b) and 55 mm long. The temperature is measured when the cutting edge cuts and closes the electrical circuit of the two K type thermocouples wires embedded in the workpieces as presented in Figure 2. Five thermocouples are positioned every 10 mm to get the transient temperature elevation. The mechanical and thermal data are recorded thanks to a NI9205 and a NI9219 cards synchronized with a NI CompacDAQ 9188 board [7].

Peer-review under responsibility of the International Scientific Committee of 7th HPC 2016 in the person of the Conference Chair Prof. Matthias Putz
doi:10.1016/j.procir.2016.04.017

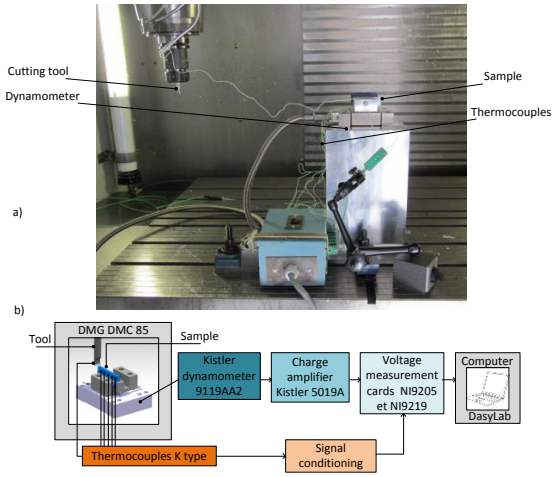

Figure 1. a) view and b) schematic of the experimental set-up.

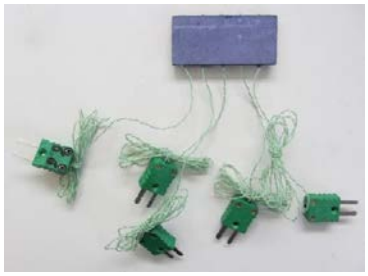

Figure 2. Thermoplastic sample with the five embedded thermocouples.

Figure 3 shows the force disturbances in the direction of the cutting speed due to the five K type thermocouples when they are cut by the tool. The force peaks are removed from the collected data to get only the values due to the studied thermoplastic material.

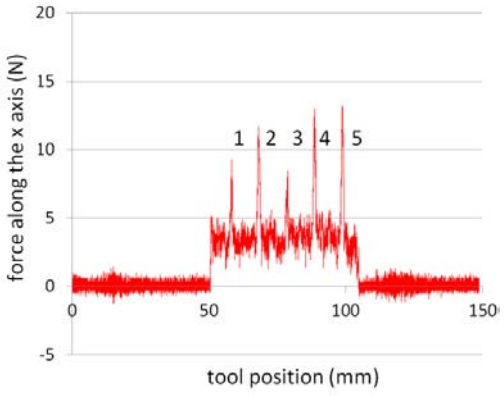

Figure 3. Disturbance on the force (F_c) along the x-axis (cutting direction) due to the cut of the thermocouples (V_c = 5m/min, h = 0.3 mm).

The cutting tool, exposed in the Figure 4 is a single edge made with K20 sintered tungsten carbide. The rake and flank angles, respectively 20° and 20°, are chosen accordingly to the industrially optimized geometry. The tool edge radius is controlled thanks to a contact profilometer to evaluate the wear and thus guaranty the results homogeneity. The parameter evolve from 4±2 µm (before the first cut) to 5±2 µm (at the end of the whole experimentation). The wear was therefore considered irrelevant.

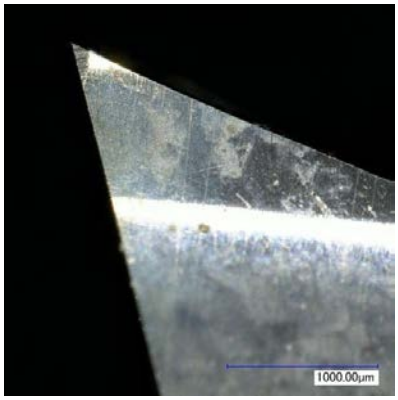

Figure 4. Side view of the tool edge.

3. Model

The model of temperature in orthogonal cutting is obtained by solving the heat equation (1) with a finite difference method coded in C++. Thanks to the spatial and temporal decomposition, equation (2) gives the temperatures on each cell thanks to the temperatures of the adjacent cells on the previous time step.

$$div(-\vec{\varphi}) + q = \rho \cdot C_p \cdot \frac{\partial T}{\partial t} \quad (1)$$

With φ the heat flux (W/m^2)

q the volumetric heat flux (W/m^3)

ρ the density (kg/m^3)

C_p the specific heat capacity (J/(kg K))

T the temperature (K)

$$(T_{i,j})_{t_{i+1}} = (T_{i,j})_{t_i} + \frac{\Delta t}{\rho\, C_p}\,[div(-\vec{\varphi}) + q] \quad (2)$$

The figure 5 describes the mesh used to solve the problem. The tool is set as fixed and the workpiece cells are continuously moving along the x direction at the cutting speed (V_c). When the chip is losing its contact with the rake face, the thermal exchange with the tool will achieve zero. The cells corresponding to the chip are thus numerically insulated from the others. In the workpiece base, as long as the tool is progressing on the sample, the material cells are ignored on the mesh. The tool removes thus a given uncut chip thickness (h). Finally cell sizes were chosen to be one sixth of the uncut chip thickness.

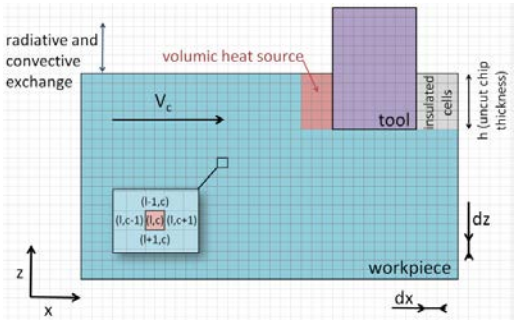

Figure 5. Schematic decomposition used for the finite difference solving.

The thermal properties (density, conductivity and heat capacity) and the boundary conditions (emissivity and exchange coefficient between materials) can be introduced in the code as thermally dependent. Literature values are used to feed the code with suitable properties. Workpiece material properties presented in table 1 are determined from industrial measurement campaign. The heat source flux is determined from the measured forces during the machining as presented in equation (3) and 90% of it are applied on the cells located upstream from the cutting edge [8]. The heat is applied on a volume ($b \cdot h \cdot h/2$) considering most of the heat is generated by plasticity in the primary shear zone and by friction on the rake face of the tool (Fig. 5).

Table 1. Properties of materials

	Tool K20 sintered tungsten carbide.	Workpiece material
λ, thermal conductivity (w/(m K))	85	0.9
ρ, density (kg/m^3)	14 500	1 800
C_p, specific heat capacity (J/(kg K))	0.0419 T + 438.87	378
ε, emissivity	0.3	23.2 T + 13.5
α, thermal expansion (m/(m·K))	$6.5 \cdot 10^{-3}$	$55 \cdot 10^{-6}$
T_g, glass transition temperature (°C)	-	140

$$W = \frac{F_x \cdot V_C}{h \cdot b} \quad (3)$$

The radiative loss on the tool and the sample are calculated from equation (4) with a given emissivity (ε) of the materials. The free convection heat flux coefficient (h_c) is estimated in equation (5) using the Mc Adams equations [9].

$$\varphi_r = \varepsilon \cdot \sigma \left({T_{room}}^4 - {T_{surface}}^4 \right) dS \quad (4)$$

$$\varphi_{conv} = h_c \left(T_{room} - T_{surface} \right) dS \quad (5)$$

Figure 6 gives an example of the results obtained by a cutting speed of 5 m/min and an uncut chip thickness of 0.5 mm. The analysis of the results shows that the thermal steady state (at 95%) is obtained after simulated 3.5 seconds of cut.

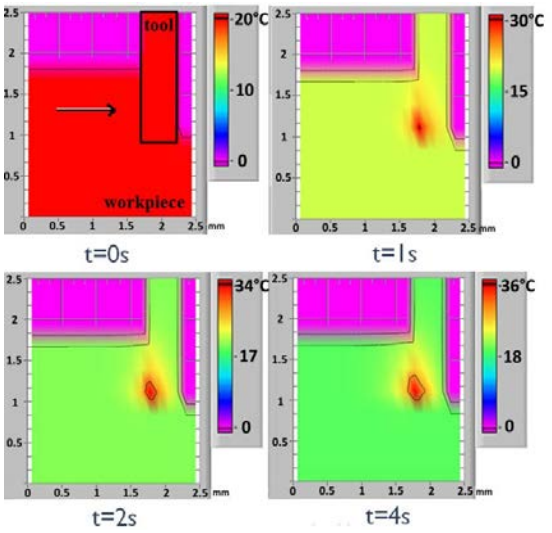

Figure 6. Simulated thermal chart (Vc = 5 m/min, h= 0.5 mm).

4. Results and discussion

With a given tool geometry (Figure 4), cutting speed and the uncut chip thickness are changed to evaluate their effects on generated cutting forces and temperature. The cutting parameters are chosen to widely cover the industrial practice. Table 2 summarized the values used for the 16 experiments. For each cutting speed, four depth of cut are investigated. Four repetitions of each conditions are performed.

Table 2. Cutting parameters levels used for the experiments.

V_c, cutting speed (m/min)	5	30	60	80
h, depth of cut (mm)	0.01	0.1	0.3	0.5

Specific cutting force (k_c) is calculated according to equation (6) to analyses the forces involved in the chip formation independently of its thickness and the width of the specimen. Figure 7 (a) shows that the specific pressure increases as the chip thickness decreases. The evolution is commonly attributed to the appearance of the plunging effect of the material when uncut chip thickness becomes close to the cutting edge radius. In metallic materials, thermal softening generally induces a decrease of k_c with the temperature increase due to the cutting speed. In thermoplastic polymers, plasticity is obtained by polymer chains sliding between themselves. As consequences, these materials viscoplastic behavior explains the increase of pressure in the Figure 7 (b) when the cutting speed increases. With a cutting speed of 80 m/min, the generated temperature in the material becomes higher than the glass transition temperature leading to the cutting forces decrease.

$$k_c = \frac{F_x}{b \cdot h} \quad (6)$$

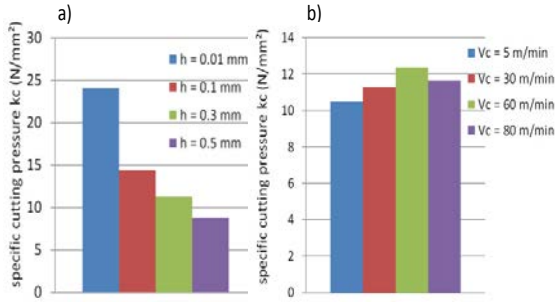

Figure 7. Simulated thermal chart : a) k_c versus h (V_c = 30 m/min) and b) k_c versus V_c (h = 0.5 mm).

Figure 8 summarizes the temperature evolutions of the tool edge versus the cutting parameters. Finite differences calculated temperatures with the cutting forces as entry are represented with the black lines in the bar graph. The temperature evaluations are 19.9 K, in mean value, lower than the measured temperatures. This difference can be explained by the fact that the model does not integrate the friction between the chip and the rake face of the tool. This localized heat source may increase locally the tool edge temperature. The finite difference resolution method also under evaluates the temperature of the interface because its considers only the temperature of the center of each cell.

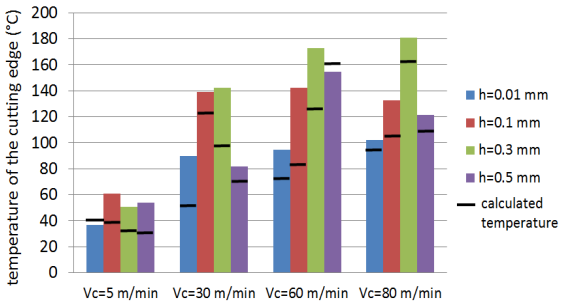

Figure 8. Evolution of the measured and calculated tool edge temperature versus uncut chip thickness and cutting speed.

5. Conclusions and outlooks

Based on known cutting forces, the finite difference model is capable to determine the temperature of the cutting edge with approximately a 20 K mean error. In order to improve the accuracy of the model, a more realistic description of the heat sources geometry has to be implemented. This has to be performed by a complete study of the frictions between the chip and the workpiece at the tool rake and flank faces. A thermal validation with thermocouples embedded in the workpiece will be needed. The finite difference calculation was firstly developed for planing as an elementary cutting operation. The same code is used to model milling operations by changing the uncut chip thickness when the tool is progressing in the workpiece material.

Acknowledgements

The authors are really grateful for the CEA Le Ripault financial support of this study.

References

[1] Davies M, Ueda T, M'Saoubi R, Mullany B, Cooke A. On The Measurement of Temperature in Material Removal Processes. CIRP Annals - Manufacturing Technology, 2007, vol. 56, n°12, p. 581-604.

[2] Rumford B. An Inquiry concerning the source of the heat which is excited by friction. Philosophical Transactions of the Royal Society of London, 1798, vol. 88, p. 80-102.

[3] Chatterjee A. Thermal degradation analysis of thermoset resins. Journal of applied polymer science, 2009, vol. 114, n°13, p. 1417-1425.

[4] Brinksmeier E, Fangmann S, Rentsch R. Drilling of composites and resulting surface integrity. CIRP Annals-Manufacturing Technology, 2011, vol. 60, n°11, p. 57-60.

[5] Kerrigan K, Thil J, Hewison R, O'Donnell G. An integrated telemetric thermocouple sensor for process monitoring of CFRP milling operations. Procedia CIRP, 2012, vol. 1, p. 449-454.

[6] Sugita N, Ishii K, Furusho T, Harada K and Mitsuishi M. Cutting temperature measurement by a micro-sensor array integrated on the rake face of a cutting tool. CIRP Annals - Manufacturing Technology, 2015, vol. 64, n°. 1, p. 77-80.

[7] Arrazola P, Ozel T, Umbrello D, Davies M, Jawahir IS. Recent advances in modelling of metal machining processes. CIRP Annals-Manufacturing Technology, 2013 vol. 62, n°12, p. 695-718.

[8] Klocke F, Brockmann M, Gierlings S, Veselovac D, Analytical model of temperature distribution in metal cutting based on Potential Theory. Mechanical Sciences, 2015, vol. 6, n°12, p. 89-94.